X-RAY DIFFRACTION

Benefits on crystallography for the analysis of the structure of Nano-powdered crystals and structure modelling simulations.

Moisés Barberá Ramos (201169840)
Department of Physics, The University of Liverpool.
16/11/2018

Abstract

X-ray diffraction applied on crystals is of great interest in the context of crystallography, being able to provide answers about the molecular structure of crystals or the identification of unknown Nano-powdered crystal substances. A 35 kV and 1 mA emission current X-ray machine analysing the lattice constant through two filters, a 2mm aperture and a Ni foil one, of an unknow sample resulted to be between (7.11 ± 0.06)Åm (1% error) and (7.16 ± 0.1)Åm (1% error), consistent with the FCC crystal KI at (7.05 ± 0.01) Åm (1% error) with a mean crystallize size of the powder at around (86.9 ± 0.9)Åm (1% error). An extensive modelling simulation of the diffraction will confirm the identification of the sample as well as providing the information about the conditions required for crystals to be BCC or FCC and why CsCl, NaCl and Kcl are classified as Simple Cubic structures.

1. Introduction

Crystals, due to their natural regularity and symmetry have been scientifically investigated for centuries [1]. Although the conclusions obtained about their structure could not be validated until the discovery of X-rays in the late 19th century when, after accepting their electromagnetic radiation form [2], started to be used as a technique to determine the structure of crystals from an atomic and molecular view. Being able to differentiate between simple cubic, body centred cubic and face centred cubic structures as shown further on.

The introduction of X-ray crystallography, the study of crystals through X-ray diffraction, was based (and still is) on the electromagnetic properties of the X-rays which, in the form of waves, reach the atoms that form the crystal and because of their electrons, the atoms scatter a portion of the X-ray's intensity as secondary circular waves through elastic scattering. Since atoms are placed in order as arrays, a group of waves will be produced adding them constructively in certain directions as described by Bragg's law [3] (equation 1).

$$2dsin(\theta) = n\lambda \qquad \text{(Eq. 1)}$$

Where n is any integer multiple of the wavelength, λ, of the beam, presenting an order of magnitude equal to that of the difference between planes, d, and θ is the incident angle that produces the scattering.

For instance, the introduction of this method demonstrated the existence of ionic compounds, later studied on this report, suggesting that not all crystals were formed by covalently bonded molecules, revealing this way some fundamental laws for material sciences [4], a mixture of physics and chemistry.

Since the periodicity of crystals offer a stronger signal than non-crystalline samples, this method is usually applied only on the first ones. Their composition out of many repeated unit cells, in three different directions (h,k,l), known as Miller indices [5], present a Fourier transform condition denoting the intensity peaks, Bragg peaks, corresponding to the exponentially growing reflections observed in the diffraction image as the scatters increase. So, each particular plane formed by the Miller indices (h,k,l,) will have a specific Bragg angle of diffraction. This constructive-like interference [6] supports the advantages of limiting this method to crystalline substances only rather than on non-crystalline ones.

In this report, we demonstrate how the use of X-ray diffraction analyses the structure of an unknown powdered sample based on the density of its electros [7], formed by an ionic

bound between a metal or NH_4 group with a halogen. By studying its intensity peaks, produced through a nickel, Ni, foil filter on the detector, as a function of the Bragg angle, will help discover the values of the lattice parameter experimentally, then checked through theoretical methods involving the Nelson-Riley function and a modelled system to reaffirm the results obtained and so, confirm the identity of the crystal sample.

In addition to this study, and in order to provide a wider insight on the analysis of the different cubic structures for crystal compounds, considering a set of atoms placed in the unit cell, the *structure factor equation* (Eq. 2) will be used to construct a spreadsheet modelling the characteristics of the selected structures and substances theoretically.

$$A_{hkl} = \sum_{i}^{n} A_i exp(iq \cdot R_i) = \sum_{i}^{n} A_i [\cos(q \cdot R_i) + i \sin(q \cdot R_i)] \quad \text{(Eq. 2)}$$

The structure factor shows that intensities of X-rays diffracted by a crystal depend on the magnitude depending on the X-ray wavelength which direction specifies the h,k,l plane of atoms, q, the positions of atoms in the unit cell of the crystal, Ri and the strength of scattering from individual atoms, Ai.

This *structure factor equation* shows that intensities of diffracted X-rays depend on magnitude from the wavelength on their specific (h,k,l)planes as well as depends on the position of the atoms and the strength of scattering from each one of them. These conditions show the main restrictions to model an accurate crystal powder diffraction simulation as shown in the results section (page: 4).

2. Results

EXPERIMENT

An X-ray PHYWE detector with a Cu x-ray tube operating at 35 kV and emitting a current of 1 mA was used throughout the progression of the experiment.

The machine was calibrated using a LiF crystal that was hit with X-rays at a set of different changing angles ranging from 8 to 45 degrees in intervals of 0.1 degrees at a speed of 1 second per interval. Analysing this scattering from the crystal with a 2mm aperture filter and with a Ni foil filter on the MEASURE software, allowed the plot of the following graph (Figure 1), showing the proper calibration by spotting two peaks at 20.4 and 22.7 degrees respectively as it should be expected for this crystal sample.

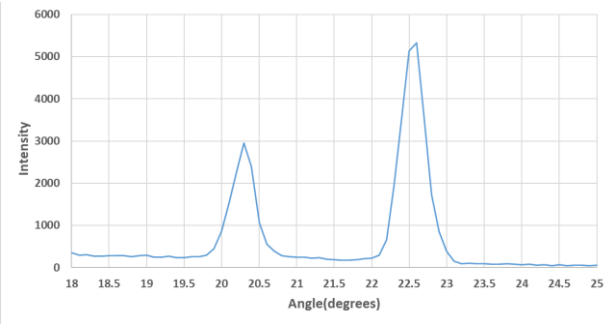

Figure 1: Graph displaying the counts against angle theta of diffraction on the LiF crystal ensuring the proper calibration of the X-ray machine spotting the peaks at the expected 20.4 and 22.7 angles.

The two filters used in the calibration, and on the rest of the experiment, give a better appreciation of the radiations involved since the 2mm aperture filter produces a higher number of records featuring alpha and beta radiation while the Ni foil filters the beta radiation and simply registers alpha interactions. These conditions, which compare by their difference in ratio angles (1.1 ratio of separation) and beta interactions producing half the intensity the alpha particles produce, will be used on the analysis to find the lattice parameter of the studied unknown sample where only the K(alpha) X-ray wavelength will reach the results this report is expecting to discern at 154 pm.

In order to proceed with the experiment and to obtain a sample to study, the grinding of an unknown crystal sample manually, during 20 minutes, reduced it to a finer powdered state and then was compressed on a metal holder with the help of a spatula to provide a smoother surface, reducing undesirable X-ray scattering while enabling a bigger amount of Bragg reflections to be observed thanks to the higher amount of particles randomly oriented.

Placing this sample as close as possible the filter on the calibrated X-ray machine and then measuring over the same range of angles as with the calibration method, but in intervals of 15 seconds per 0.1 degree rotated. The observations from this sample, studied through the 2mm aperture filter and the Ni foil filter, are shown in the figure 2, where it is perceptible

the differences that each filter present as discussed before.

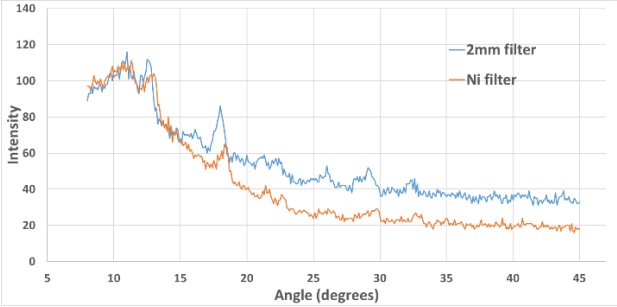

Figure 2: Showing the Brag peaks of the unknown crystal sample on the range from 8 to 45 degrees using both, the 2mm filter and the Ni foil filter, making observable the comparisons between both of them, the Ni filter shifted on a ratio of 1.1 against the 2mm one as well as presenting a lower intensity due to the filtration of beta particles which have half the intensity of alfa particles.

After acquiring the information of each of the points describing the graph above, a simple MATLAB program (code showed on the appendix) could be constructed to select the different peak intervals (fig. 12 and 13 on the appendix) and then use those intervals to find with the "Curve Fitting Tool" application, using the Gaussian equation (Eq. 3) to fit their curve, the exact angle at which each Bragg peak is placed on the graph and, consequently, its error.

$$Gaussian\ eq. = a1 \cdot e^{-\left(\frac{x-b1}{c1}\right)^2} + d \qquad \text{(Eq. 3)}$$

Where a1 is the intensity, b1 is the angle at that point, c1 is a given value by the app which will then be used to find the FWHM and d is the background.

Proceeding on finding the identity of the sample studied, and once all data collection has already been performed, a series of equations are used to go from those Bragg peaks found to the experimental lattice parameter.

From each of the two data sets, from the Ni foil filter and the 2mm aperture one, the theta values and their errors are given so they are first transformed from radians to the degrees scale and the square of their sinus is calculated. This allows to plot a graph where this sinus squared is presented against the non-decimal multiplier N, as seen in figure 3 and 4, which has been calculated after multiplying the ratio of the sinus square by some integer that provides a closer integer value for every ratio value so it can then be used to find the Miller indices (h,k,l) since $h^2 + k^2 + l^2 = N$, tables 1 and 2 on the appendix followed with the error calculation at each step.

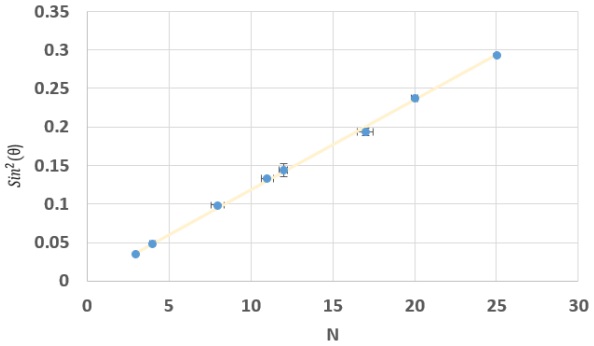

Figure 3: Graph plotting sin square of theta as a function of the exact integer N from the observations with the Ni foil filter on the X-ray machine. Features a line of best fit that is consistent with the errors found.

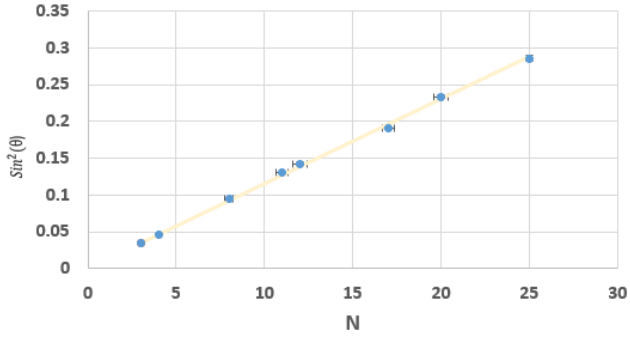

Figure 4: Graph plotting sin square of theta as a function of the exact integer N from the observations with the 2mm aperture filter on the X-ray machine. Features a line of best fit that is consistent with the errors found.

The lattice parameter depends only on the K(α) values so the graph from the Ni foil filter are the ones used to calculate its value since, as explained before, this foil filters the beta counts. Using the JLineFit software is an efficient method to find the gradient of the graph which will give the data to calculate the lattice parameter, a, from the equation 4.

$$Sin^2(\theta) = \frac{\lambda^2}{4a^2} \cdot N \qquad \text{(Eq. 4)}$$

Where, as observed on the graph, the $Sin^2(\theta)$ are the y-axis values, the N is the x-axis values and the $\frac{\lambda^2}{4a^2}$ is the gradient that will be used to find a, the lattice parameter, by rearranging the wavelength, λ, and the rest of constants as seeing on the next equation 5.

$$a = \sqrt{\frac{\lambda^2}{4 \cdot gradient}} \qquad \text{(Eq. 5)}$$

And the error explained on equation 14 on the appendix.

This process gives a result for the lattice constant of (7.11 ± 0.06)Åm, armstrongs meter, (1% error) which by comparing the lattice constant table [8] and checking the substances' lattice constants the (7.05 ± 0.01)Åm (0.1% error) KI is the only substance consistent with our results since it agrees with the consistency check, equation 6 conditions where X_1 is the calculated value, X_2 is the real value and ΔX_1 and ΔX_2 are their respective errors.

$$|X_1 - X_2| < 3\sqrt{\Delta X_1{}^2 + \Delta X_2{}^2} \qquad \text{(Eq. 6)}$$

To provide a more accurate analysis of the results, the Nelson-Riley (NR) function shows the value of the lattice parameter, a, as the intercept of plotting the NR function, equation 7, (where the error comes from the derivative of the NR function over the derivative of theta times the error on theta) against the apparent value of *a* for each specific Bragg peak, figure 5, from following Bragg's law, equation 1, where d is $\sqrt{\frac{a^2}{N}}$.

$$NR = \frac{1}{2}\left(\frac{\cos(\theta)^2}{\sin(\theta)} \cdot \frac{\cos(\theta)^2}{\theta}\right) \qquad \text{(Eq. 7)}$$

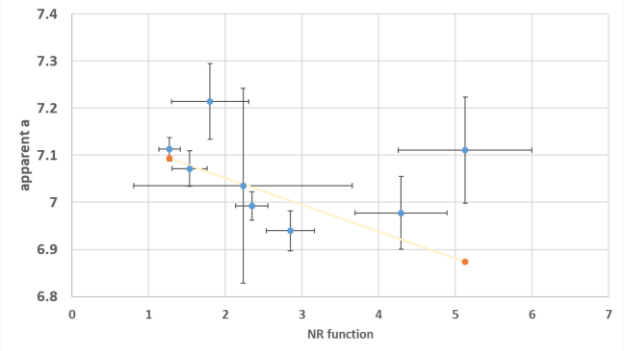

Figure 5: Graph plotting the apparent values of the lattice parameter on the y- axis against the results obtained from the NR function for each Bragg peak. Includes error bars and a line of best fit to determine the accuracy of the results. The bigger error bars approximate the best fit line to a straight line [9] which also shows a method with less accuracy.

Using the JLineFit software this time to calculate the intercept of the graph shows a result for the lattice parameter of (7.16 ± 0.1)Åm (1% error) which is more consistent with the substance NH_4I with a lattice parameter of (7.24 ± 0.01)Åm (0.1%) [8].

This Nelson-Riley function process is a straighter forward method to find the result of the lattice parameter but, as seeing on the figure 5, presents a bigger inaccuracy than the standard method described to find the first result.

Since both experimental methods show a higher consistency with two different substances then a theoretical approach must be considered. Crystals can be mainly divided in simple cubic, body centred cubic (BCC) and face centred cubic (FCC) structures. The presence of an odd multiplier to find N on our data analysis classifies our unknown sample as a face centred cubic crystal [11] and the structures of the KI and NH_4I substances detected on our processes are FCC and BCC structure respectively [11] what eliminates NH_4I from the possibility of being the unknown sample and leaving us with the discovery of KI as the identity of the crystal investigated.

To find a better understanding of X-ray crystallization, after finding the identity of the sample studied, it's crystallized size can be calculated since the size of the crystallites in the powder provoke the Bragg peak. And to do so, the Scherrer equation (Eq. 8) can be used to estimate the mean crystallized size, L, where the wavelength, λ, the cosine of theta is in degrees and the full width at half maximum (FWHM) of the Bragg peak, is represented as β. β is the result of calculating $2\sqrt{2\ln(2)} \cdot c1$ where c1 is the value given from the "Curve Fitting Tool" application in MATLAB for each Bragg peak as seeing on equation 3.

$$L = \frac{0.9\lambda}{2\beta\cos(\theta)} \qquad \text{(Eq. 8)}$$

And the error is shown in the appendix, equation 17.

Calculating the mean for each value of L and the standard deviation over the square root of the number of events to find the error leads a result for the mean crystallize size of the powder of (86.9 ± 0.9)Åm (1% error) from the Ni filter study and a result of (83.9 ± 4.5)Åm (6% error) from the 2mm aperture filter study. These results are consistent with the expectations we could have since the studied sample is composed of nano crystals what makes the order of magnitude match as well as couple with the approximately 1 armstrong meters, Åm, of distance between atoms.

MODELLING

- **KI**

Based on a theoretical approach, the studied sample, identified as a KI substance with a face centred cubic structure, presents 8 atoms with atomic numbers 19 and 53 for the K and I elements respectively since the metal, K, is a cation while the halogen, I, is an anion. This information can be used to model where the Bragg peaks are going to be spotted as a function of normalised intensity versus the angle theta.

For each of the 8 atoms from the h, k and l planes they will record a result for all three axis (x, y and z) they are involved in, using the structure factor equation as reference, equation 2.

Where the value for each x as a function of each combination of planes, q·r, comes from equation 9:

$$q \cdot r = 2\pi(hx + ky + lz) \qquad \text{(Eq. 9)}$$

While for the y and z values the cosine and sine of q·r was calculated respectively.

This set of information was combined with the K and I ions' atomic number to find the amplitude of the waves scattered on each plane, equation 20, and by squaring the amplitude get its intensity for each plane. Consequently, the value of theta can be found with the help of the Miller indices of each plane as well as using the lattice parameter of this sample, 7.05 Åm, as the wavelength of 1.54 Åm and so on the number a certain value of theta has been repeated on the theta column, known as the theta index of multiplicity, θ Index Mult, [12]. Continuing with the wide range of steps on the modelling of this experiment, the Lorentz-Polarisation, LP, factor, equation 10, accounts for the angle-dependence scattering of x-rays

$$LP = \frac{1}{\theta^{\frac{5}{2}}} \qquad \text{(Eq. 10)}$$

And adding the values of each theta variable for a particular plane combination with LP, will provide the intensity at each Bragg angle we were looking for, which after normalising it could then be plotted as a function of each Bragg angle expressed in degrees, table 8.

This modelling featuring 124 plane combinations produced a theoretical expectation of Bragg peaks, considering the KI substance as the unknown studied sample, that could be compared with the obtained experimental ones as shown on table 1 and figure 6 for a better visual understanding of the results.

THEORETICAL PEAKS		EXPERIMENTAL PEAKS	
hkl	theta	hkl	theta
1.1.1.	10.9	1.1.1.	10.8
2.0.0.	12.6	2.0.0.	12.8
2.2.0.	18.0	2.2.0.	18.3
3.1.1.	21.2	3.1.1.	21.4
2.2.2.	22.2	2.2.2.	22.3
4.1.0.	26.8	4.1.0.	26.1
4.2.0.	29.2	4.2.0.	29.1
4.3.0.	33.1	4.3.0.	32.8

Table 1: Comparing the Bragg peaks at theta with the planes they were spotted at in the experimental and theoretical (modelled) procedure. As seen, for the same combination of Miller indices, approximately the same value of theta is assigned what helps ensure KI as the real identity of the sample studied.

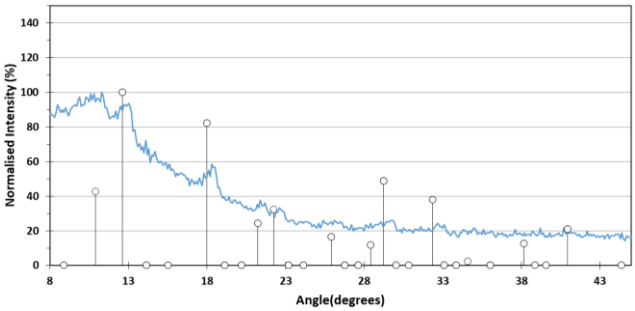

Figure 6: Graph comparing the modelled Bragg peaks, plotting the normalized intensity versus the angle theta, for the KI substance which matches the recordings for the unknown powdered crystal on the X-ray machine ensuring the correctness when identifying KI as the identity of the studied sample.

After observing the accuracy of this method on the study of crystals a series of different modelling were proposed in order to offer a more extensive understanding of crystal's characteristics by going across examples of all three kinds of structure: simple cubic, BCC and FCC.

- **Simple cubic, BCC and FCC study**

Following the previous approach, we constructed a group of crystal structures by placing atoms of elements in the unit cell, so it was possible to simulate diffraction from the different structures we want to analyse thanks to the structure factor equation (Eq. 2).

BCC

To study the body centred cubic structure a single element for a more straight-forward analysis of this condition is used. With two atoms, a single atom visualised on the middle of a unit cell (with coordinates x, y and z equal to 0.5 each) and an eighth of an atom visualised at each of the eight corners of this cube that added up generate the totality of 2 atoms in the model.

The results this analysis is expecting to find follow the rules for BCC structures that the single element will present all its hkl squared values adding up a totality of an even number. This means that from all the combinations of planes, only those for which summing each squared Miller index equals an even number ($h^2 + k^2 + l^2 = even\ N$) will generate a Bragg peak on the intensity over angle theta graph.

This main rule, and so the modelling performed, shows the lowest value of N to be 2 (Table 2), since any value lower than that is odd and then would be breaking the rule for BCC crystal structure.

			Atom 1			Atom 2			θ (deg)	$I_{rel}(\theta)$
			x	y	z	x	y	z		
h	k	l	0	0	0	0.5	0.5	0.5		Normalised
			q*R	cos(q*R)	sin(q*R)					
0	0	0	0	1	0	0.0	1.0	0.0	0.0	0.0
0	0	1	0	1	0	3.1	-1.0	0.0	6.7	0.0
0	0	2	0	1	0	6.3	1.0	0.0	13.5	20.8
0	0	3	0	1	0	9.4	-1.0	0.0	20.5	0.0
0	0	4	0	1	0	12.6	1.0	0.0	27.9	3.4
0	1	0	0	1	0	3.1	-1.0	0.0	6.7	0.0
0	1	1	0	1	0	6.3	1.0	0.0	9.5	100.0
0	1	2	0	1	0	9.4	-1.0	0.0	15.1	0.0
0	1	3	0	1	0	12.6	1.0	0.0	21.7	25.5
0	1	4	0	1	0	15.7	-1.0	0.0	28.8	0.0
0	2	0	0	1	0	6.3	1.0	0.0	13.5	20.8
0	2	1	0	1	0	9.4	-1.0	0.0	15.1	0.0

Table 2: Showing the first 12 plane combinations of the BCC modelling, out of the 124, and the values for each coordinate as represented for the structure factor equation components highlighted on blue and highlighting on green the position of the highest Bragg peak placed on the lowest N value 2, as discussed, corresponding to the 011 plane hkl.

Plotting the intensities of all plane combinations against their angle theta show the diffraction of the body centered cubic structure study for a single element, figure 7.

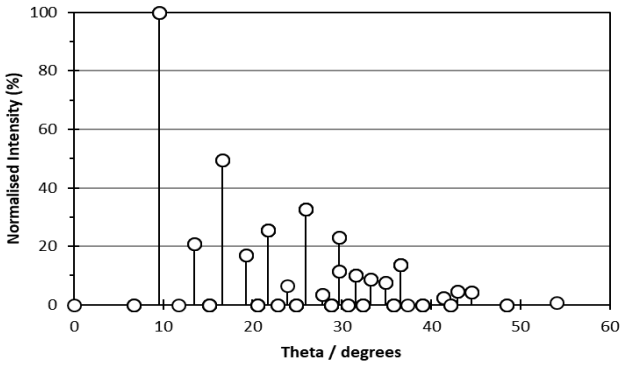

Figure 7: Graph showing the diffraction simulation of a single element BCC crystal with lattice parameter 6.59Åm and X-ray wavelength 1.54Åm. It plots the normalized intensity against the angle theta in degrees.

FCC

To study the face centered cubic structure 4 atoms are present in the unit cell, half atom is placed at the center of each of the 6 walls of the cube which adds up to 3 while the fourth atom comes from, as in the BCC structure, the addition of all eighths of an atom placed at each of the eight corners of the cube together.

The same simulation used for the BCC structure, with lattice constant 6.59Åm and 1.54Åm wavelength, is used now but for four atoms instead, showing how the first main Bragg peak, intensity of 100, is at the plane combination 111 for hkl. This behaves as expected for the rule of FCC structures that explain that hkl values must be all even or all odd and for that rule 111 is the first plane combination at which that happens, fail to do so would result on an intensity of 0 and so, no Bragg peak at that plane combination, Table 3 and figure 8.

			Atom 1			...	Atom 4			θ (deg)	$I_{rel}(\theta)$
			x	y	z	...	x	y	z		
h	k	l	0	0	0	...	0.5	0.5	0		Normalised
			q*R	cos(q*R)	sin(q*R)	...					
0	0	0	0	1	0	...	0	1	0	0	0
0	0	1	0	1	0	...	0.0	1.0	0.0	6.7	0
0	0	2	0	1	0	...	0.0	1.0	0.0	13.5	52.0
0	0	3	0	1	0	...	0.0	1.0	0.0	20.5	0
0	0	4	0	1	0	...	0.0	1.0	0.0	27.9	8.5
0	1	0	0	1	0	...	3.1	-1.0	0.0	6.7	0
1	0	4	0	1	0	...	3.1	-1.0	0.0	28.8	0
1	1	0	0	1	0	...	6.3	1.0	0.0	9.5	0
1	1	1	0	1	0	...	6.3	1.0	0.0	11.7	100.0
1	1	2	0	1	0	...	6.3	1.0	0.0	16.6	0
1	1	3	0	1	0	...	6.3	1.0	0.0	22.8	56.3
1	1	4	0	1	0	...	6.3	1.0	0.0	29.7	0

Table 3: Showing a set of 12 plane combinations of the FCC modelling with four atoms, out of the 124 plane combinations, and the value for their coordinates following the structure factor equation components highlighted in blue and highlighting with green the position of the highest Bragg peak when the first hkl plane combination reflects all odd numbers 111. When this rule for FCC structured crystals is not met, we then can observe an intensity of 0 in those planes.

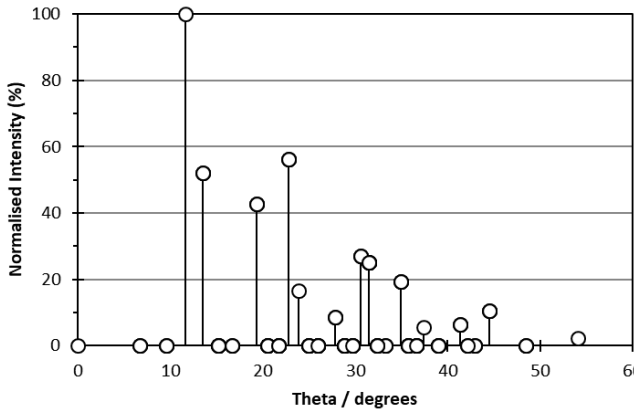

Figure 8: Graph showing the diffraction simulation of an FCC crystal with lattice parameter 6.59Åm and X-ray wavelength 1.54Åm. It plots the normalized intensity against the angle theta in degrees.

SIMPLE CUBIC

Studying Simple Cubic structures required the same modelling but a different approach since this time, a set of three different crystals was chosen (CsCl, NaCl, KCl) and, by analyzing the results, they were classified Simple Cubic since none of them followed the BCC nor FCC requirements.

1. CsCl

Cesium chloride seems to follow the same structure as BCC since its disposition is the same as that of a BCC crystal on the unit cell. Although, since there are two different atoms rather than a single one and the metal element is not alpha iron, tungsten, chromium nor beta titanium [13], then it cannot be a BCC.

In this case, the ions Cs^+ and Cl^- (atomic numbers 53 and 19 respectively) are considered to build the modelling where, as the electron charge interact with the X-rays, the strength of scattering of an atom will be proportional to the number of electrons.

The results from this process, despite featuring two atoms the same way a BCC does, it generates a different modelling due to the different atomic numbers incorporated in the calculations and the different lattice parameter now assigned as 4.1Åm for CsCl, table 4 and figure 9.

			Atom 1			Atom 2			θ (deg)	$I_{real}(\theta)$
			x	y	z	x	y	z		
h	k	l	0	0	0	0.5	0.5	0.5		Normalised
			q*R	cos(q*R)	sin(q*R)					
0	0	0	0	1	0	0	1.0	0	0	0
0	0	1	0	1	0	3.1	-1.0	0	6.7	26.7
0	0	2	0	1	0	6.3	1.0	0	13.5	20.8
0	0	3	0	1	0	9.4	-1.0	0	20.5	3.3
0	0	4	0	1	0	12.6	1.0	0	27.9	3.4
0	1	0	0	1	0	3.1	-1.0	0	6.7	26.7
0	1	1	0	1	0	6.3	1.0	0	9.5	100.0
0	1	2	0	1	0	9.4	-1.0	0	15.1	13.9
0	1	3	0	1	0	12.6	1.0	0	21.7	25.5
0	1	4	0	1	0	15.7	-1.0	0	28.8	4.2
0	2	0	0	1	0	6.3	1.0	0	13.5	20.8
0	2	1	0	1	0	9.4	-1.0	0	15.1	13.9

Table 4: Showing the first 12 plane combinations of the Simple Cubic modelling, out of the 124, for its both atoms and the values for each coordinate as represented for the structure factor equation components highlighted on blue and highlighting on green the position of the highest Bragg peak where despite it is found on the same hkl plane of 011 as expected for a BCC crystal, CsCl fails to include any of the metal elements identified above.

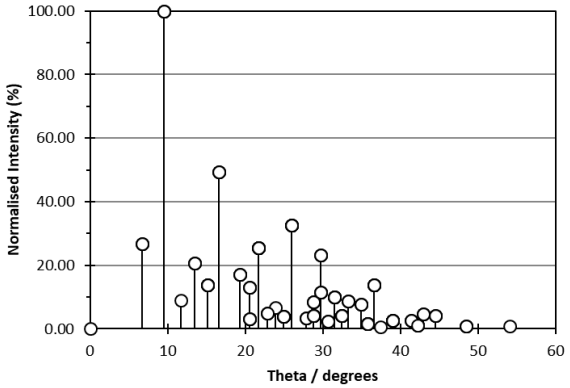

Figure 9: Graph showing the diffraction simulation of a Simple Cubic crystal with lattice parameter 4.1Åm and X-ray wavelength 1.54Åm. It plots the normalized intensity against angle theta in degrees for the CsCl substance.

2. NaCl

Sodium Chloride presents eight atoms and a structure formed by two FCC where one is shifted as 0.5 from the other what makes this one an expansion of the FCC modelling accounting for the ionic bounding of Na^+ and Cl^- (atomic numbers 10 and 18 respectively).

Presenting two FCC crystals together and shifted produces a destructive interference that reduces the maximum Bragg peak from its 111 plane to the lowest all even numbers. 002, and every hkl plane combination with one 2 and two 0s, is then the plane combination at which the maximum intensity should be found, table 5, and is because of this destructive interference that the NaCl substance can be structured as a set of simple cubic structures all grouped together [14].

			Atom 1			...	Atom 8			θ (deg)	$I_{real}(\theta)$
			x	y	z	...	x	y	z		
h	k	l	0	0	0	...	1	0.5	0		Normalised
			q*R	cos(q*R)	sin(q*R)	...					
0	0	0	0	1	0	...	0	1	0	0	0
0	0	1	0	1	0	...	0	1	0	7.9	0
0	0	2	0	1	0	...	0	1	0	15.9	100.0
0	0	3	0	1	0	...	0	1	0	24.2	0
0	0	4	0	1	0	...	0	1	0	33.2	15.8
0	1	0	0	1	0	...	3.1	-1	0	7.9	0
0	1	1	0	1	0	...	3.1	-1	0	11.2	0
0	1	2	0	1	0	...	3.1	-1	0	17.8	0
0	1	3	0	1	0	...	3.1	-1	0	25.6	0
0	1	4	0	1	0	...	3.1	-1	0	34.3	0
0	2	0	0	1	0	...	6.3	1	0	15.9	100.0
0	2	1	0	1	0	...	6.3	1	0	17.8	0

Table 5: Showing the first 12 plane combinations of the Simple Cubic modelling, out of the 124, for its eight atoms and the values for each coordinate as represented for the structure factor equation components highlighted on blue and highlighting on green the position of the highest Bragg peak where due to the destructive interference they are reduced from an expected 111 plane combination to the lowest plane which Miller indices are all even, so they are 002, 020 and later 200.

The resultant diffraction simulated for the NaCl substance is shown on figure 10.

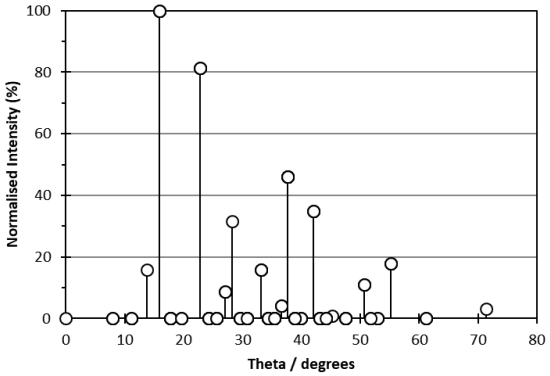

Figure 10: Graph showing the diffraction simulation of a Simple Cubic crystal with lattice parameter 5.6Åm and X-ray wavelength 1.54Åm. It plots the normalized intensity against angle theta in degrees for the NaCl substance.

3. KCl

Potassium Chloride is the last of the three selected chlorides selected and presents the same structure as NaCl with the difference that K^+ AND Cl^- have the same atomic number 18, what means all atoms have the same size. This particular disposition when calculating the modeling table since I will follow the same steps as table 5 apart from the difference in the lattice parameter and the atomic numbers used to find the amplitude.

The highest intensity will keep being found on the lowest all even plane combinations as in NaCl so that again confirms the Simple Cubic structure for KCl since the destructive interference is present again.

So, the simulated diffraction for this crystal can be represented as follows, figure 11:

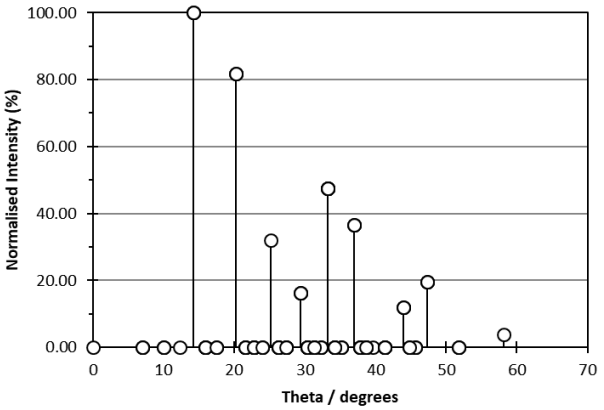

Figure 11: Graph showing the diffraction simulation of a Simple Cubic crystal with lattice parameter 6.28Åm and X-ray wavelength 1.54Åm. It plots the normalized intensity against angle theta in degrees for the KCl substance.

3. Discussion

Being able to find the identity of an unknown crystal sample as well as analyzing its structure through X-ray crystallization is the prove the efficiency of using X-rays diffraction as a method to study crystals in a way firstly suggested on the 17th century [1] but couldn't be reached until the discovery of X-rays on the 19th century [19].

On the results section for the modelling, when studying the different structures, it was seeing how when atoms where in phase and no destructive interference took place the Bragg's law, equation 1, was satisfied while for the destructive interference there was another element out of phase forming a new crystal.

The different three structures studied on the length of this report show an appreciation on how the matter is distributed through space allowing atoms to be closer or further from each other. For instance, the BCC covers a 68% of the space for each original unit cell and the FCC rises that space up to 74.04%, producing denser matter in comparison with those structures presenting a Simple Cubic unit cell that only covers a 52%.

Preparing the crystal powder on the chemical laboratory could lead to wrong results if not performed properly, that's why the supervision of an experienced assistant was required to ensure the grinding of the, at the beginning, unknown crystal sample was reduced to a proper nano-powder state, which is reached after an average of 20 minutes of manual grinding, and then compacted on a holder

showing a smooth surface to reduce the undesirable scattering X-rays that would interact with wrongly oriented particles if a rougher surface is left on the holder.

The calibration method shown on page 2 reduces the possibilities for shifted-angle values on the results obtained and to avoid a lower level of recordings through the filter, the sample was always placed the closest possible to the aperture so the X-rays from the Cu X-ray tube after being reflected on the sample don't get lost with the surroundings.

To find the identity of the crystal sample, finding the lattice parameter was needed and the errors to do so were carried from those on the theta angle given from the MATLAB program and investigated on the "Curve Fitting" tool and in the following steps calculated through mathematical operations as shown on the appendix. The efficiency of the X-ray machine will determine the accuracy of the angle theta values recorded, which are considered under the calculations of the MATLAB program. All the processes followed were based on a theoretical model, table 6, which was easily calculated using a lab manual [15] and where no errors were assigned, these could then be found on the experimental procedure as seeing on figures 3 and 4.

theta	sin(theta)	sin2(theta)	ratio	Multiplied ratio	N	(hkl)
13.90	0.24	0.06	1.00	3.00	3	111
16.10	0.28	0.08	1.33	4.00	4	200
23.10	0.39	0.15	2.67	8.00	8	220
27.20	0.46	0.21	3.62	10.86	11	311
28.73	0.48	0.23	4.00	12.01	12	222
33.73	0.56	0.31	5.34	16.03	16	400
37.22	0.60	0.37	6.34	19.02	19	331

Table 6: Showing the theoretical approach to plot a sin squared graph as a function of the multiplier N to later find the lattice constant and so the identity of the sample to study. This is the process in which the result operations where based for the identification of KI on page 3 but without considering any error.

The error on the gradient still depends on the mathematical operations undertaken so little human error is found on this process where, when comparing the results obtained with the lattice parameters expected [16] the error on those ones was given up to two significant figures. This simulation corresponds then to the AgCl sample since the simulated lattice constant equals to (5.54 ± 0.01)Åm (0.1% error) in consistency with the expected (5.55 ± 0.01)Åm (0.1% error).

The Nelson-Riley functions keeps depending on theta as before, equation 6, and so the error sources are based on the logical order of significant figures again based on the error calculations showed in the appendix.

Consequently, for all modelled data on this report, since it's based on given samples, the errors will appear for the already values of the lattice parameter [16] and wavelength of X-rays [17].

These sources of error affected on our results by adding a margin of miscalculation that appear to make our results consistent with the expected, equation 5, ensuring the proper conclusions to be found although by reducing the precision.

4. Conclusions

X-ray crystallography is a scientific method to study the structure and identity of crystals by analyzing the diffraction produced by Cu X-rays reflecting on the surface of an unknow powdered sample through an Ni foil aperture filter, filtering K(β) radiation, and a 2mm aperture filter generating a shifted data set by a 1.1 ratio from the previous one.

As studied on this dissertation, data recorded through those two filters after hitting the sample with X-rays on a range of angles from 8 to 45 degrees on intervals of 0.1 degrees every 15 seconds produced the needed data to calculate the lattice parameter (found on the Ni Filter since only K(α) radiation was required) at (7.11 ± 0.06)Åm, armstrongs meter, (1% error) and using the same data, but analysing the intercept of the Nelson-Riley function, Eq. 7, instead of the gradient of figure 3, the resultant lattice parameter, a, was found at (7.16 ± 0.1)Åm (1% error). Since both results were consistent with two different crystal substances, a theoretical study showed that since our unknown sample had an odd multiplier N, its structure must be FCC and so, the only consistent face centred cubic substance [8] with our results was the KI crystal with a lattice constant of (7.05 ± 0.01)Åm (0.1% error). Confirmed to be the right identity of the crystal powder after doing a modelling of the theoretical expected Bragg peaks and seeing the concordance between the modelled and experimental results on table 1 and figure 6.

Results complimented with the findings of the mean crystallize size for the studied sample ranging between (86.9 ± 0.9)Åm (1% error) from the Ni filter study and (83.9 ± 4.5)Åm (6% error) from the 2mm aperture study.

Developing a simulated diffraction modelling is an accurate method to study the structure of known crystals without the need of acquiring the data though experimentation. The study of the selected three chlorides: CsCl, NaCl and KCl, using the explained modelling tables on page 5 and 6, showed how CsCl had two different atoms placed in a structure similar to the BCC one but since the atoms were different instead of being the same and the metal involved did not couple with the body centered cubic requirements then its structure only matched that of a Simple Cubic. Following with the next two crystals, the NaCl and KCl have the same structure, two FCC structures together with one of them being shifted by 0.5 from the origin. This position of the 8 atoms causes a destructive interference reducing the expected point at which the highest Brag peak would be expected and so it breaks the face centerd cubic conditions. Both can then be explained as a series of Simple cubic cells all added together and so that's the structure of NaCl and KCl (which features the same size for all its atoms since their anions and cations have 18 as atomic number).

Studying the BCC and FCC structures following the same modelling lead to observe how the BCC, with two atoms, for a single element must satisfy the condition in which the sum of the square of all three Miller indices must be equal to an even number for it to feature a Bragg peak, which implies that the lowest hkl plane combination will be equal to 2, spotted first on the plane 011 (and any combination of this three digits) as seeing on table 2.

On the other hand, the FCC structure study, with four atoms, required all the Miller indices to be all ever or all odd for them to spot a Bragg peak and so, the lowest plane combination at which that happens, showing the highest Bragg peak, is when the hkl planes equal 111 as seeing on table 3. Fail to follow this rule would result on the intensity equal 0 and so no Bragg peak detected for that plane combination.

When analyzing the structure of crystals, the electron density of the molecules interacting with X-rays will produce the information of the atomic positions that then describe the molecular structure of the crystal.

5. References

[1] Schneer, Cecil: "Kepler's New Year's Gift of a Snowflake." Isis, Volume 51, No. 4. University of Chicago Press, 1960, pp. 531–545.

[2] von Laue, Max. "My Development as a Physicist; AN AUTOBIOGRAPHY". *International Union of CRYSTALLOGRAPHY*. International Union of CRYSTALLOGRAPHY.

[3] Bragg, W.H.; Bragg, W.L. (1913). "The Reflexion of X-rays by Crystals". *Proc. R. Soc. Lond. A*. **88** (605):42838. Bibcode:1913RSPSA..88..428B. doi:10.1098/rspa.1913.0040.

[4] E. Maire & P. J. Withers (2014) Quantitative X-ray tomography, International Materials Reviews, 59:1, 1-43, DOI: 10.1179/1743280413Y.0000000023

[5] Neil W. Ashcroft and N. David Mermin, Solid State Physics (Harcourt: New York, 1976)

[6] *Interferometry*, Cambridge University Press, Cambridge, WH Steel, 1986.

[7] https://www.um.edu.mt/__data/assets/pdf_file/0019/93025/X-Ray_Crystallography.pdf (visited 17/11/2018)

[8] https://vital.liv.ac.uk/webapps/blackboard/execute/content/file?cmd=view&content_id=_1688019_1&course_id=_791491_1 (visited during the extension of the full experiment)

[9] https://vital.liv.ac.uk/webapps/blackboard/execute/content/file?cmd=view&content_id=_1688020_1&course_id=_791491_1 (visited 14/11/2018)

[10] Processing and Properties of Compound Semiconductors, AnnamrajuKasi Viswanath, 2001.

[11] https://materials.springer.com/ (visited 13/11/2018)

[12] https://vital.liv.ac.uk/webapps/blackboard/exec

ute/content/file?cmd=view&content_id=_1688040_1&course_id=_791491_1 (page 28)

[13] https://www.corrosionpedia.com/definition/1593/body-centered-cubic-bcc(Visited 16/11/2018)

[14] Elements of Modern X-ray Physics, 2nd Ed. by Jens Als-Nielsen and Des McMorrow, John Wiley & Sons, Ltd., 2011

[15] https://vital.liv.ac.uk/webapps/blackboard/execute/content/file?cmd=view&content_id=_1688040_1&course_id=_791491_1 (page 32)

[16] CRC Handbook of Chemistry and Physics, 72nd Edition Ed. D.R. Lide, CRC Press, 1991.

[17] http://www.science.unitn.it/~fisica1/raggi_x/siti/xraywwwserver/xray%20wwwserver.htm (Visited 17/11/2018)

[18] Novelize, Robert. *Squire's Fundamentals of Radiology*. Harvard University Press. 5th edition. 1997. ISBN 0-674-83339-2 p. 1.

[19] *"Crystal Structures" General Chemistry: Principles & Modern Applications, ninth Edition. New Jersey: Pearson Education, Inc., Petrucci, Ralph H., William S. Harwood, F. Geoffrey Herring, and Jeffry D. Madura. 2007. 501-508*

Appendix A: Error Calculations

theta	error	sin(theta)	error	sin2(theta)	error	ratio	Multiplied	N	error	(hkl)
10.81	0.17	0.188	0.003	0.035	0.001	1	3.0	3	0	111
12.75	0.14	0.221	0.002	0.049	0.001	1.4	4.2	4	0.15	200
18.29	0.11	0.314	0.002	0.098	0.001	2.8	8.4	8	0.40	220
21.42	0.09	0.365	0.002	0.133	0.001	3.8	11.4	11	0.37	311
22.28	0.64	0.379	0.011	0.144	0.008	4.1	12.3	12	0.26	222
26.11	0.28	0.440	0.005	0.194	0.004	5.5	16.5	17	0.48	410
29.14	0.15	0.487	0.003	0.237	0.003	6.7	20.2	20	0.22	420
32.77	0.11	0.541	0.002	0.293	0.002	8.3	25.0	25	0.01	430

Table 7: Table with the modelling X-ray diffraction for the angles, theta, recorded from the Ni foil aperture filter. It has the same structure as the theoretical one shown in the discussion section for AgCl but this one features the errors and later on the appendix the explanation of where these errors come from.

Error on theta, θ:
-Given from performing the MATLAB program seen below. And given in radians.

Error sin(θ):

$$\Delta \sin(\theta) = \sin(\Delta\theta) \qquad \text{(Eq. 11)}$$

Error $\sin^2(\theta)$:

$$\Delta\sin^2(\theta) = 2 \cdot \left(\frac{\Delta \sin(\theta)}{\sin(\theta)}\right) \cdot \sin^2(\theta) \qquad \text{(Eq. 12)}$$

Error on N:

$$\Delta N = |multiplied\ ratio - N| \qquad \text{(Eq. 13)}$$

Error on the lattice parameter, a, from the gradient:

$$\Delta a = \frac{\Delta gradient}{gradient} \cdot a \qquad \text{(Eq. 14)}$$

To obtain a from the NR function, first the apparent a for each angle was found, and the error corresponds to:

$$\Delta apparent\ a = \frac{\Delta\sin(\theta)}{\sin(\theta)} \cdot apparent\ a \qquad \text{(Eq. 15)}$$

And the error on the NR function following the error function for a single variable:

$$\Delta NR = \frac{1}{2}\left(\frac{cos^2(\theta)}{\theta} + \cos(\theta) \cdot \cot(\theta)\right) \cdot \Delta\theta \text{(Eq. 16)}$$

Finally, the error on the lattice parameter obtained from the Intercept from the NR function method is the same as the error on the intercept which is provided on the JLineFit software.
On the study of the mean crystallize size of the sample, the error on equation 8 is:

$$\Delta L = \sqrt{\frac{\Delta\beta}{\beta} + \frac{\Delta\cos(\theta)}{\cos(\theta)}} \cdot L \qquad \text{(Eq. 17)}$$

Where $\Delta\beta$ comes from the error on equation for FWHM:

$$\beta = FWHM = 2\sqrt{2\ln(2)} \cdot c1 \quad \text{(Eq. 18)}$$

Since the error on C1 is a given value from the MATLAB program below:

$$\Delta\beta = \frac{\Delta c1}{c1} \cdot \beta \quad \text{(Eq. 19)}$$

And finally, the error on the mean for the mean crystallize size if the standard deviation on the mean over the square root of elements on the mean.

Appendix B:

$\lvert A_{hkl}\rvert$	I_{hkl}	θ (rad)	θ Mult	θ Index Mult	LP	$I_{real}(\theta)$	θ (deg)	$I_{real}(\theta)$ Normalised
288	82944	#DIV/0!	1	1	0	0	#DIV/0!	0
1.76E-14	3.11E-28	0.109438	3	2	252.3933	4.71E-25	6.2703458	2.15533E-30
288	82944	0.220215	3	2	43.94215	21868428	12.617407	100
5.29E-14	2.8E-27	0.333825	6	2	15.53108	5.22E-25	19.126783	2.38732E-30
288	82944	0.452127	3	2	7.275283	3620646	25.904946	16.5565
1.76E-14	3.11E-28	0.109438	3	2	252.3933	4.71E-25	6.2703458	2.15533E-30
0	0	0.155081	3	4	105.5852	0	8.8854912	0
1.76E-14	3.11E-28	0.246718	6	4	33.07473	2.47E-25	14.135922	1.12978E-30

Table 8: Showing the order of the steps followed to complete the modelling of any of the theoretical models calculated on this report. This one particularly corresponds to the KI study.

The amplitude is the first step on this process and was found from calculating, equation 20:

$$\lvert A_{hkl}\rvert = \sqrt{\left(\sum_i y_i \cdot atomic\ number_1 + \sum_i z_i \cdot atomic\ number_2\right)^2}$$

MATLAB peak intervals observation

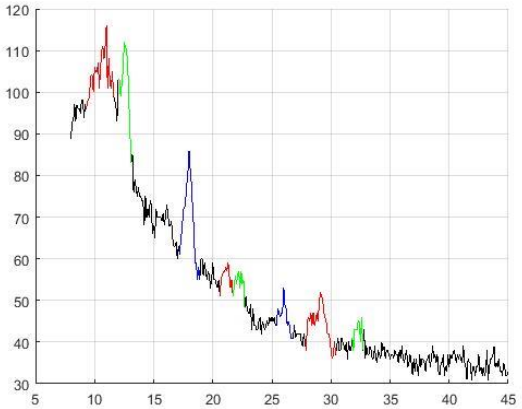

Figure 12: Plot constructed on MATLAB featuring, with different colors, the intervals at which each Bragg peak could be spotted using the 2mm aperture filter on a range from 8 to 45 degrees.

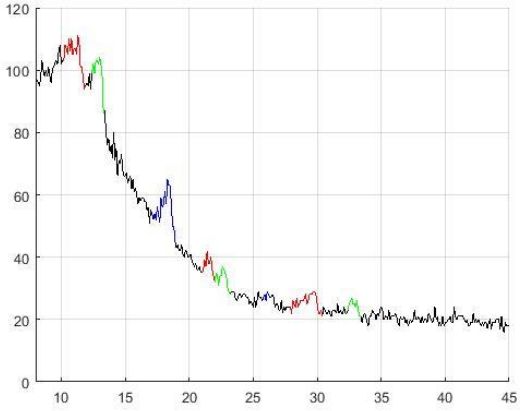

Figure 13: Plot constructed on MATLAB featuring, with different colors, the intervals at which each Bragg peak could be spotted using the Ni foil filter on a range from 8 to 45 degrees.

MATLAB SCRIPT

```
%MOISES BARBERA RAMOS
%13/11/2018
%data analysis

clear all
close all
clc
%FILTER 2mm

M = csvread('2mm filter day 2.csv')

%PEAK 1

theta1 = M(14:37,1);
I1 = M(14:37,2);

%PEAK 2

theta2 = M(41:52, 1);
I2 = M(41:52, 2);

%PEAK 3

theta3 = M(93:110, 1);
I3 = M(93:110, 2);

%PEAK 4

theta4 = M(127:138, 1);
I4 = M(127:138, 2);

%PEAK 5

theta5 = M(138:148, 1);
I5 = M(138:148, 2);

%PEAK 6
```

```
theta6 = M(175:189, 1);
I6 = M(175:189, 2);

%PEAK 7

theta7 = M(200:225, 1);
I7 = M(200:225, 2);

%PEAK 8

theta8 = M(239:248, 1);
I8 = M(239:248, 2);

%NIQUEL filter

Ni = csvread('Ni filter day 2.csv')

%2PEAK 1

ntheta1 = Ni(23:40,1);
nI1 = Ni(23:40,2);

%2PEAK 2

ntheta2 = Ni(45:55, 1);
nI2 = Ni(45:55, 2);

%2PEAK 3

ntheta3 = Ni(93:110, 1);
nI3 = Ni(93:110, 2);

%2PEAK 4

ntheta4 = Ni(130:141, 1);
nI4 = Ni(130:141, 2);

%2PEAK 5

ntheta5 = Ni(141:153, 1);
nI5 = Ni(141:153, 2);

%2PEAK 6

ntheta6 = Ni(178:185, 1);
nI6 = Ni(178:185, 2);

%2PEAK 7

ntheta7 = Ni(200:225, 1);
nI7 = Ni(200:225, 2);

%2PEAK 8

ntheta8 = Ni(245:255, 1);
nI8 = Ni(245:255, 2);
```

```
figure(1)
hold on
plot(Ni(:,1),Ni(:,2),'k-');
plot(ntheta1,nI1,'r-');
plot(ntheta2,nI2,'g-');
plot(ntheta3,nI3,'b-');
plot(ntheta4,nI4,'r-');
plot(ntheta5,nI5,'g-');
plot(ntheta6,nI6,'b-');
plot(ntheta7,nI7,'r-');
plot(ntheta8,nI8,'g-');
hold off

grid on

xlim([min(Ni(:,1)) max(Ni(:,1))]);


figure(2)

plot(1:length(Ni(:,2)),Ni(:,2),'k-');

figure(3)
hold on
plot(M(:,1),M(:,2),'k-');
plot(theta1,I1,'r-');
plot(theta2,I2,'g-');
plot(theta3,I3,'b-');
plot(theta4,I4,'r-');
plot(theta5,I5,'g-');
plot(theta6,I6,'b-');
plot(theta7,I7,'r-');
plot(theta8,I8,'g-');
hold off

grid on

figure(4)

plot(1:length(M(:,2)),M(:,2),'k-');
```

Access to the EXCEL spreadsheets to check all calculations is open through the following link leading to a DROPBOX folder storing the spreadsheets for everyone to access no matter where you are.

https://www.dropbox.com/sh/1oatz5uzjmnv2fo/AAC5Jp1Sq7MKaVRT_QROcHgQa?dl=0